

Search for Lepton Flavor Violation in $\Upsilon(3S) \rightarrow e^\pm \mu^\mp$

J. P. Lees,¹ V. Poireau,¹ V. Tisserand,¹ E. Grauges,² A. Palano,³ G. Eigen,⁴ D. N. Brown,⁵ Yu. G. Kolomensky,⁵ M. Fritsch,⁶ H. Koch,⁶ T. Schroeder,⁶ R. Cheaib,⁷ C. Hearty,⁷ T. S. Mattison,⁷ J. A. McKenna,⁷ R. Y. So,⁷ V. E. Blinov,⁸ A. R. Buzykaev,⁸ V. P. Druzhinin,⁸ V. B. Golubev,⁸ E. A. Kozyrev,⁸ E. A. Kravchenko,⁸ A. P. Onuchin,^{8,*} S. I. Serednyakov,⁸ Yu. I. Skovpen,⁸ E. P. Solodov,⁸ K. Yu. Todyshev,⁸ A. J. Lankford,⁹ B. Dey,¹⁰ J. W. Gary,¹⁰ O. Long,¹⁰ A. M. Eisner,¹¹ W. S. Lockman,¹¹ W. Panduro Vazquez,¹¹ D. S. Chao,¹² C. H. Cheng,¹² B. Echenard,¹² K. T. Flood,¹² D. G. Hitlin,¹² J. Kim,¹² Y. Li,¹² D. X. Lin,¹² S. Middleton,¹² T. S. Miyashita,¹² P. Ongmongkolkul,¹² J. Oyang,¹² F. C. Porter,¹² M. Röhrken,¹² Z. Huard,¹³ B. T. Meadows,¹³ B. G. Pushpawela,¹³ M. D. Sokoloff,¹³ L. Sun,^{13,†} J. G. Smith,¹⁴ S. R. Wagner,¹⁴ D. Bernard,¹⁵ M. Verderi,¹⁵ D. Bettoni,¹⁶ C. Bozzi,¹⁶ R. Calabrese,¹⁶ G. Cibinetto,¹⁶ E. Fioravanti,¹⁶ I. Garzia,¹⁶ E. Luppi,¹⁶ V. Santoro,¹⁶ A. Calcaterra,¹⁷ R. de Sangro,¹⁷ G. Finocchiaro,¹⁷ S. Martellotti,¹⁷ P. Patteri,¹⁷ I. M. Peruzzi,¹⁷ M. Piccolo,¹⁷ M. Rotondo,¹⁷ A. Zallo,¹⁷ S. Passaggio,¹⁸ C. Patrignani,^{18,‡} B. J. Shuve,¹⁹ H. M. Lacker,²⁰ B. Bhuyan,²¹ U. Mallik,²² C. Chen,²³ J. Cochran,²³ S. Prell,²³ A. V. Gritsan,²⁴ N. Arnaud,²⁵ M. Davier,²⁵ F. Le Diberder,²⁵ A. M. Lutz,²⁵ G. Wormser,²⁵ D. J. Lange,²⁶ D. M. Wright,²⁶ J. P. Coleman,²⁷ E. Gabathuler,^{27,*} D. E. Hutchcroft,²⁷ D. J. Payne,²⁷ C. Touramanis,²⁷ A. J. Bevan,²⁸ F. Di Lodovico,^{28,§} R. Sacco,²⁸ G. Cowan,²⁹ Sw. Banerjee,³⁰ D. N. Brown,^{30,¶} C. L. Davis,³⁰ A. G. Denig,³¹ W. Gradl,³¹ K. Griessinger,³¹ A. Hafner,³¹ K. R. Schubert,³¹ R. J. Barlow,^{32,**} G. D. Lafferty,³² R. Cenci,³³ A. Jawahery,³³ D. A. Roberts,³³ R. Cowan,³⁴ S. H. Robertson,³⁵ R. M. Seddon,³⁵ N. Neri,³⁶ F. Palombo,³⁶ L. Cremaldi,³⁷ R. Godang,^{37,††} D. J. Summers,^{37,*} P. Taras,³⁸ G. De Nardo,³⁹ C. Sciacca,³⁹ G. Raven,⁴⁰ C. P. Jessop,⁴¹ J. M. LoSecco,⁴¹ K. Honscheid,⁴² R. Kass,⁴² A. Gaz,⁴³ M. Margoni,⁴³ M. Posocco,⁴³ G. Simi,⁴³ F. Simonetto,⁴³ R. Stroili,⁴³ S. Akar,⁴⁴ E. Ben-Haim,⁴⁴ M. Bomben,⁴⁴ G. R. Bonneaud,⁴⁴ G. Calderini,⁴⁴ J. Chauveau,⁴⁴ G. Marchiori,⁴⁴ J. Ocariz,⁴⁴ M. Biasini,⁴⁵ E. Manoni,⁴⁵ A. Rossi,⁴⁵ G. Batignani,⁴⁶ S. Bettarini,⁴⁶ M. Carpinelli,^{46,‡‡} G. Casarosa,⁴⁶ M. Chruszcz,⁴⁶ F. Forti,⁴⁶ M. A. Giorgi,⁴⁶ A. Lusiani,⁴⁶ B. Oberhof,⁴⁶ E. Paoloni,⁴⁶ M. Rama,⁴⁶ G. Rizzo,⁴⁶ J. J. Walsh,⁴⁶ L. Zani,⁴⁶ A. J. S. Smith,⁴⁷ F. Anulli,⁴⁸ R. Faccini,⁴⁸ F. Ferrarotto,⁴⁸ F. Ferroni,^{48,§§} A. Pilloni,⁴⁸ G. Piredda,^{48,*} C. Büniger,⁴⁹ S. Dittrich,⁴⁹ O. Grünberg,⁴⁹ M. Heß,⁴⁹ T. Leddig,⁴⁹ C. Voß,⁴⁹ R. Waldi,⁴⁹ T. Adye,⁵⁰ F. F. Wilson,⁵⁰ S. Emery,⁵¹ G. Vasseur,⁵¹ D. Aston,⁵² C. Cartaro,⁵² M. R. Convery,⁵² J. Dorfan,⁵² W. Dunwoodie,⁵² M. Ebert,⁵² R. C. Field,⁵² B. G. Fulsom,⁵² M. T. Graham,⁵² C. Hast,⁵² W. R. Innes,^{52,*} P. Kim,⁵² D. W. G. S. Leith,^{52,*} S. Luitz,⁵² D. B. MacFarlane,⁵² D. R. Muller,⁵² H. Neal,⁵² B. N. Ratcliff,⁵² A. Roodman,⁵² M. K. Sullivan,⁵² J. Va'vra,⁵² W. J. Wisniewski,⁵² M. V. Purohit,⁵³ J. R. Wilson,⁵³ A. Randle-Conde,⁵⁴ S. J. Sekula,⁵⁴ H. Ahmed,⁵⁵ M. Bellis,⁵⁶ P. R. Burchat,⁵⁶ E. M. T. Puccio,⁵⁶ M. S. Alam,⁵⁷ J. A. Ernst,⁵⁷ R. Gorodeisky,⁵⁸ N. Guttman,⁵⁸ D. R. Peimer,⁵⁸ A. Soffer,⁵⁸ S. M. Spanier,⁵⁹ J. L. Ritchie,⁶⁰ R. F. Schwitters,⁶⁰ J. M. Izen,⁶¹ X. C. Lou,⁶¹ F. Bianchi,⁶² F. De Mori,⁶² A. Filippi,⁶² D. Gamba,⁶² L. Lanceri,⁶³ L. Vitale,⁶³ F. Martinez-Vidal,⁶⁴ A. Oyanguren,⁶⁴ J. Albert,⁶⁵ A. Beaulieu,⁶⁵ F. U. Bernlochner,⁶⁵ G. J. King,⁶⁵ R. Kowalewski,⁶⁵ T. Lueck,⁶⁵ I. M. Nugent,⁶⁵ J. M. Roney,⁶⁵ R. J. Sobie,⁶⁵ N. Tasneem,⁶⁵ T. J. Gershon,⁶⁶ P. F. Harrison,⁶⁶ T. E. Latham,⁶⁶ R. Prepost,⁶⁷ and S. L. Wu⁶⁷

(The BABAR Collaboration)

¹Laboratoire d'Annecy-le-Vieux de Physique des Particules (LAPP),
Université de Savoie, CNRS/IN2P3, F-74941 Annecy-Le-Vieux, France

²Universitat de Barcelona, Facultat de Física, Departament ECM, E-08028 Barcelona, Spain

³INFN Sezione di Bari, I-70126 Bari, Italy

⁴University of Bergen, Institute of Physics, N-5007 Bergen, Norway

⁵Lawrence Berkeley National Laboratory and University of California, Berkeley, California 94720, USA

⁶Ruhr Universität Bochum, Institut für Experimentalphysik 1, D-44780 Bochum, Germany

⁷Institute of Particle Physics^a; University of British Columbia^b, Vancouver, British Columbia, Canada V6T 1Z1

⁸Budker Institute of Nuclear Physics SB RAS, Novosibirsk 630090^a,
Novosibirsk State University, Novosibirsk 630090^b,
Novosibirsk State Technical University, Novosibirsk 630092^c, Russia

⁹University of California at Irvine, Irvine, California 92697, USA

¹⁰University of California at Riverside, Riverside, California 92521, USA

¹¹University of California at Santa Cruz, Institute for Particle Physics, Santa Cruz, California 95064, USA

- ¹²California Institute of Technology, Pasadena, California 91125, USA
- ¹³University of Cincinnati, Cincinnati, Ohio 45221, USA
- ¹⁴University of Colorado, Boulder, Colorado 80309, USA
- ¹⁵Laboratoire Leprince-Ringuet, Ecole Polytechnique, CNRS/IN2P3, F-91128 Palaiseau, France
- ¹⁶INFN Sezione di Ferrara^a; Dipartimento di Fisica e Scienze della Terra, Università di Ferrara^b, I-44122 Ferrara, Italy
- ¹⁷INFN Laboratori Nazionali di Frascati, I-00044 Frascati, Italy
- ¹⁸INFN Sezione di Genova, I-16146 Genova, Italy
- ¹⁹Harvey Mudd College, Claremont, California 91711, USA
- ²⁰Humboldt-Universität zu Berlin, Institut für Physik, D-12489 Berlin, Germany
- ²¹Indian Institute of Technology Guwahati, Guwahati, Assam, 781 039, India
- ²²University of Iowa, Iowa City, Iowa 52242, USA
- ²³Iowa State University, Ames, Iowa 50011, USA
- ²⁴Johns Hopkins University, Baltimore, Maryland 21218, USA
- ²⁵Université Paris-Saclay, CNRS/IN2P3, IJCLab, F-91405 Orsay, France
- ²⁶Lawrence Livermore National Laboratory, Livermore, California 94550, USA
- ²⁷University of Liverpool, Liverpool L69 7ZE, United Kingdom
- ²⁸Queen Mary, University of London, London, E1 4NS, United Kingdom
- ²⁹University of London, Royal Holloway and Bedford New College, Egham, Surrey TW20 0EX, United Kingdom
- ³⁰University of Louisville, Louisville, Kentucky 40292, USA
- ³¹Johannes Gutenberg-Universität Mainz, Institut für Kernphysik, D-55099 Mainz, Germany
- ³²University of Manchester, Manchester M13 9PL, United Kingdom
- ³³University of Maryland, College Park, Maryland 20742, USA
- ³⁴Massachusetts Institute of Technology, Laboratory for Nuclear Science, Cambridge, Massachusetts 02139, USA
- ³⁵Institute of Particle Physics^a; McGill University^b, Montréal, Québec, Canada H3A 2T8
- ³⁶INFN Sezione di Milano^a; Dipartimento di Fisica, Università di Milano^b, I-20133 Milano, Italy
- ³⁷University of Mississippi, University, Mississippi 38677, USA
- ³⁸Université de Montréal, Physique des Particules, Montréal, Québec, Canada H3C 3J7
- ³⁹INFN Sezione di Napoli and Dipartimento di Scienze Fisiche, Università di Napoli Federico II, I-80126 Napoli, Italy
- ⁴⁰NIKHEF, National Institute for Nuclear Physics and High Energy Physics, NL-1009 DB Amsterdam, The Netherlands
- ⁴¹University of Notre Dame, Notre Dame, Indiana 46556, USA
- ⁴²Ohio State University, Columbus, Ohio 43210, USA
- ⁴³INFN Sezione di Padova^a; Dipartimento di Fisica, Università di Padova^b, I-35131 Padova, Italy
- ⁴⁴Laboratoire de Physique Nucléaire et de Hautes Energies, Sorbonne Université, Paris Diderot Sorbonne Paris Cité, CNRS/IN2P3, F-75252 Paris, France
- ⁴⁵INFN Sezione di Perugia^a; Dipartimento di Fisica, Università di Perugia^b, I-06123 Perugia, Italy
- ⁴⁶INFN Sezione di Pisa^a; Dipartimento di Fisica, Università di Pisa^b; Scuola Normale Superiore di Pisa^c, I-56127 Pisa, Italy
- ⁴⁷Princeton University, Princeton, New Jersey 08544, USA
- ⁴⁸INFN Sezione di Roma^a; Dipartimento di Fisica, Università di Roma La Sapienza^b, I-00185 Roma, Italy
- ⁴⁹Universität Rostock, D-18051 Rostock, Germany
- ⁵⁰Rutherford Appleton Laboratory, Chilton, Didcot, Oxon, OX11 0QX, United Kingdom
- ⁵¹IRFU, CEA, Université Paris-Saclay, F-91191 Gif-sur-Yvette, France
- ⁵²SLAC National Accelerator Laboratory, Stanford, California 94309 USA
- ⁵³University of South Carolina, Columbia, South Carolina 29208, USA
- ⁵⁴Southern Methodist University, Dallas, Texas 75275, USA
- ⁵⁵St. Francis Xavier University, Antigonish, Nova Scotia, Canada B2G 2W5
- ⁵⁶Stanford University, Stanford, California 94305, USA
- ⁵⁷State University of New York, Albany, New York 12222, USA
- ⁵⁸Tel Aviv University, School of Physics and Astronomy, Tel Aviv, 69978, Israel
- ⁵⁹University of Tennessee, Knoxville, Tennessee 37996, USA
- ⁶⁰University of Texas at Austin, Austin, Texas 78712, USA
- ⁶¹University of Texas at Dallas, Richardson, Texas 75083, USA
- ⁶²INFN Sezione di Torino^a; Dipartimento di Fisica, Università di Torino^b, I-10125 Torino, Italy
- ⁶³INFN Sezione di Trieste and Dipartimento di Fisica, Università di Trieste, I-34127 Trieste, Italy
- ⁶⁴IFIC, Universitat de Valencia-CSIC, E-46071 Valencia, Spain
- ⁶⁵Institute of Particle Physics^a; University of Victoria^b, Victoria, British Columbia, Canada V8W 3P6
- ⁶⁶Department of Physics, University of Warwick, Coventry CV4 7AL, United Kingdom
- ⁶⁷University of Wisconsin, Madison, Wisconsin 53706, USA

We report on the first search for electron-muon lepton flavor violation (LFV) in the decay of a b quark and b antiquark bound state. We look for the LFV decay $\Upsilon(3S) \rightarrow e^\pm \mu^\mp$ in a sample of 118 million $\Upsilon(3S)$ mesons from 27 fb⁻¹ of data collected with the BABAR detector at the SLAC

PEP-II e^+e^- collider operating with a 10.36 GeV center-of-mass energy. No evidence for a signal is found and we set a limit on the branching fraction $\mathcal{B}(\Upsilon(3S) \rightarrow e^\pm\mu^\mp) < 3.6 \times 10^{-7}$ at 90% CL. This result can be interpreted as a limit $\Lambda_{NP}/g_{NP}^2 > 80$ TeV on the energy scale Λ_{NP} divided by the coupling-squared g_{NP}^2 of relevant new physics.

PACS numbers: 11.30.j, 11.30.Fs, 13.20.Gd, 13.20.v, 14.40.Gx, 14.40.n, 14.60.-z, 14.60.Cd, 14.60.Ef, 14.65.Fy

In the standard model (SM), the three lepton flavors (electron, muon, tau) are carried by the charged leptons (e^- , μ^- , and τ^-) and their associated neutrinos (ν_e , ν_μ , ν_τ). Were it not for the fact that neutrinos oscillate from one flavor to another, lepton flavor would be strictly conserved in all reactions in the SM. Although mixing between the neutrino flavor eigenstates permits charged lepton flavor violating (LFV) processes at higher-order, these are extremely suppressed in the SM by powers of the small neutrino masses. Therefore, observation of charged LFV would be a clear signature of new physics (NP), and placing experimentally stringent limits on the branching fractions of such processes tightly constrains NP models. Searches for electron-tau and muon-tau LFV in decays of bound states of a b quark and b antiquark ($b\bar{b}$) have yielded no evidence of a signal and upper limits ranging from 3.1×10^{-6} to 6.0×10^{-6} on their branching fractions have been set [1]. This paper describes the first search for electron-muon LFV in the decay of a $b\bar{b}$ bound-state.

Indirect theoretical constraints on LFV decays of vector (i.e., spin = 1, parity = -1) $b\bar{b}$ bound states (referred to as the $\Upsilon(nS)$ mesons, $n = 1, 2, 3, 4, \dots$) can be derived using an argument based on the non-observation of LFV decays of the muon in conjunction with unitarity considerations [2]. In these calculations, it is assumed that a virtual Υ meson could potentially contribute to the muon LFV decay. The most stringent indirect bound on electron-muon LFV decays of the $\Upsilon(3S)$ (with mass $M_{\Upsilon(3S)} = 10.36$ GeV) obtained in this way is $\mathcal{B}(\Upsilon(3S) \rightarrow e^\pm\mu^\mp) \leq 2.5 \times 10^{-8}$, which uses the reported limit on the branching fraction $\mathcal{B}(\mu \rightarrow 3e) < 1.0 \times 10^{-12}$ [3]. Using LFV limits from μ - e conversions, Ref. [4] sets an upper bound at 3.9×10^{-6} . However, it has been noted in Ref. [2] that the size of the vector boson exchange contribution to the $\mu \rightarrow 3e$ decay amplitude can be significantly reduced if there are kinematical suppressions. Such suppressions are possible when the effective vector boson couplings involve derivatives (or momentum factors). This possibility means there could be effective tensor and pseudo-tensor LFV couplings in the $\mu \rightarrow 3e$ decay, which would reduce the contribution of virtual $\Upsilon(nS)$ bosons as they only have vector couplings. Reference [2] estimates that the contribution of the virtual $\Upsilon(3S) \rightarrow e^\pm\mu^\mp$ to the $\mu \rightarrow 3e$ rate would be reduced by approximately $M_\mu^2/(2M_{\Upsilon(3S)}^2)$, leading to a re-calculated bound on $\mathcal{B}(\Upsilon(3S) \rightarrow e^\pm\mu^\mp) \leq 1 \times 10^{-3}$. The measurement we report here is several orders of magnitude more sensitive than this indirect limit. We use our result

to place constraints on Λ_{NP}/g_{NP}^2 of NP processes that include LFV, where g_{NP} is the coupling of the NP and Λ_{NP} is the energy scale of the NP.

Our sample of $\Upsilon(3S)$ meson data was collected with the *BABAR* detector at the PEP-II asymmetric-energy e^+e^- collider at the SLAC National Accelerator Laboratory. The detector was operated from 1999 to 2008 and collected data at the center-of-mass (CM) energies of the $\Upsilon(4S)$ (10.58 GeV), $\Upsilon(3S)$ (10.36 GeV), and $\Upsilon(2S)$ (10.02 GeV) resonances, as well as at energies in the vicinity of these resonances. In this paper we describe a direct search for LFV decays in a sample of 122 million $\Upsilon(3S)$ decays corresponding to an integrated luminosity of 27.96 ± 0.17 fb $^{-1}$ [5] collected during 2008 (referred to as Run 7). Data collected at the $\Upsilon(4S)$ in 2007 (referred to as Run 6) with an integrated luminosity of 78.31 ± 0.35 fb $^{-1}$ [5], data taken 40 MeV below the $\Upsilon(4S)$ resonance corresponding to 7.752 ± 0.036 fb $^{-1}$ [5], and data taken 40 MeV below the $\Upsilon(3S)$ resonance corresponding to 2.623 ± 0.017 fb $^{-1}$ [5] constitute control samples. These are used to evaluate non-resonant contributions to the background and to study systematic effects in a signal-free sample. We employ a blind analysis strategy [6] in which 0.93 fb $^{-1}$ of the $\Upsilon(3S)$ sample is used solely in the stage prior to unblinding, during which selection criteria are optimized and all systematic uncertainties evaluated. The data sample reserved for the LFV search is based on $(117.7 \pm 1.2) \times 10^6$ $\Upsilon(3S)$ decays, corresponding to 27.02 ± 0.16 fb $^{-1}$, and excludes the 0.93 fb $^{-1}$ sample.

In the *BABAR* detector, which is described in detail elsewhere [7, 8], the trajectories of charged particles are measured in a 5-layer silicon vertex tracker (SVT) surrounded by a 40-layer cylindrical drift chamber (DCH). This charged particle tracking system is inside a 1.5 T solenoid with its field running approximately parallel to the e^+e^- beams and together they form a magnetic spectrometer. In order to identify and measure the energies and directional information of photons and electrons, an electromagnetic calorimeter (EMC) composed of an array of 6580 thallium doped CsI crystals, located just inside the superconducting magnet, is used. Muons and neutral hadrons are identified by arrays of resistive plate chambers or limited streamer-tube detectors inserted into gaps in the steel of the Instrumented Flux Return (IFR) of the magnet. The $\Upsilon(4S)$ control sample data for this analysis are restricted to Run 6 to ensure that the control (Run 6) and signal (Run 7) data sets have the same IFR detector configurations following an IFR upgrade program that

was completed prior to the beginning of Run 6.

The signature for $\Upsilon(3S) \rightarrow e^\pm \mu^\mp$ events consists of exactly two oppositely charged primary particles, an electron and a muon, each with an energy close to half the total energy of the e^+e^- collision in the CM frame, E_B . There are two main sources of background: (i) $e^+e^- \rightarrow \mu^+\mu^-(\gamma)$ events in which one of the muons is misidentified, decays in flight, or generates an electron in a material interaction; and (ii) $e^+e^- \rightarrow e^+e^-(\gamma)$ events in which one of the electrons is misidentified. Background from $e^+e^- \rightarrow \tau^+\tau^- \rightarrow e^\pm \mu^\mp 2\nu 2\bar{\nu}$ is efficiently removed with the kinematic requirements described below. Generic $\Upsilon(3S)$ decays to two charged particles where there is particle misidentification are also a potential background.

The $\Upsilon(4S)$ Run 6 data, which is at a CM energy above the $\Upsilon(3S)$ mass, is used as a high statistics control sample to estimate the continuum, i.e., non- $\Upsilon(3S)$, background in Run 7 data. Although collected at the $\Upsilon(4S)$ resonance, because the large width of the $\Upsilon(4S) \rightarrow B\bar{B}$ strong decays suppresses the branching fractions of lepton-pair $\Upsilon(4S)$ decays as well as any potential LFV decays, Run 6 data provides a reliable continuum control sample. The KK2F Monte Carlo (MC) generator [9] is used to simulate μ -pair and τ -pair events. The BH-WIDE generator [10] is used to simulate Bhabha events. Both generators take into account initial- and final-state radiation. They also are used to cross-check the Run 6 data-driven estimates of the continuum background. The EvtGen generator [11] is used to simulate hadronic continuum events and generic $\Upsilon(3S)$ decays, as well as the signal $\Upsilon(3S) \rightarrow e^\pm \mu^\mp$ decays, in which the electron and muon have a $(1 + \cos^2 \theta)$ distribution, where θ is the CM polar angle relative to the e^- beam. The simulated μ -pair, τ -pair and generic $\Upsilon(3S)$ samples correspond to approximately twice the number of events expected in the $\Upsilon(3S)$ data set, while the Bhabha sample corresponds to approximately half the number of events. The GEANT4 [12] suite of programs is used to simulate the response of the *BABAR* detector.

Event selection proceeds in two stages. In the first stage, a dedicated $e\mu$ filter is used to preselect events with only an electron candidate and a muon candidate in the detector. In this filter all events, in addition to passing either the drift chamber or electromagnetic calorimeter higher level triggers, are required to have exactly two tracks of opposite charge that are separated by more than 90° in the CM. One of the tracks must pass a very loose electron selection ($E/p > 0.8$) and the other a very loose muon requirement ($E/p < 0.8$), where E is the energy deposited in the EMC associated with the track of momentum p . The preselection has an 80% efficiency for signal events, including geometrical acceptance. The first row in Table I documents this preselection efficiency along with the numbers of background events expected from generic $\Upsilon(3S)$ decays, as predicted by EvtGen, and the

amount of background from the continuum as determined by the Run 6 data control sample. It also includes the number of events preselected from the unblinded $\Upsilon(3S)$ data sample.

TABLE I: Impact of each component of the selection on the signal efficiency, number of background events, and number of events in the data. The first row provides information on the pre-selection. The last row provides the information after applying all selection criteria. Rows 2 to 7 provide information when all requirements are applied except the criterion associated with the particular row. The luminosity-normalized expected number of events in the third and fourth columns are the background events from the generic $e^+e^- \rightarrow \Upsilon(3S)$ MC and the data-driven continuum background events estimated from the $e^+e^- \rightarrow \Upsilon(4S)$ sample, respectively. The last column represents the number of events in the $\Upsilon(3S)$ data sample after unblinding.

Selection Criterion	Signal Efficiency (%)	$\Upsilon(3S)$ BG	Continuum BG	Events in Data
Pre-Selec.	80.20 ± 0.12	75516 ± 180	725003 ± 500	945480
Optimized PID	50.74 ± 0.15	5180 ± 50	320910 ± 330	358322
2 tracks in final state	23.54 ± 0.13	0	14.1 ± 2.2	18
Lep. Mom.	26.84 ± 0.12	87 ± 6	253 ± 9	302
Back-to-back	24.02 ± 0.13	0.5 ± 0.5	36 ± 6	39
EMC Accept.	24.95 ± 0.13	0	13.5 ± 2.2	17
Energy on EMC	24.52 ± 0.13	0	16.9 ± 2.4	19
All Criteria	23.42 ± 0.13	0	12.2 ± 2.1	15

In the second stage of the analysis, we apply tighter and optimized particle identification (PID) and kinematic criteria. Applying PID to select events with one muon and one electron is the most effective means of reducing the background while maintaining an acceptable efficiency. All components of the *BABAR* detector contribute to PID. Different PID selectors have been developed by *BABAR* to distinguish each particle type in a set of multivariate analyses. These are described in more detail in Ref. [8]. Selectors for this analysis based on error-correcting output codes [13] and decision trees are used to identify electrons, pions, and kaons, whereas bagged decision tree selectors [14] are used to identify muons. The selectors can be deployed to provide different nested levels of particle efficiency and background, from “Super Loose” (most efficient, least pure) to “Super Tight” (least efficient, most pure), where candidates selected by tighter criteria of the selector are a subset of

events that pass looser selection criteria. We optimize the choice of the electron and muon selectors to maximize $\varepsilon_{e\mu}/\sqrt{1+N_{BG}}$, where $\varepsilon_{e\mu}$ is the final efficiency as determined from signal MC, and N_{BG} is the number of expected background events as predicted by data control samples in Run 6 and generic $\Upsilon(3S)$ MC events. In the optimized selection, electron candidates are required to pass the ‘‘Super Tight’’ electron selector and muon candidates to pass the ‘‘Tight’’ muon selector. In addition, electron candidates are required to fail the ‘‘Tight’’ muon selector and muons are required to fail the ‘‘Super Tight’’ electron selector. Each track is also required to fail the ‘‘Loose’’ pion selector as well as the ‘‘Loose’’ kaon selector.

Kinematic requirements are also applied to suppress $e^+e^- \rightarrow \tau^+\tau^- \rightarrow e^\pm\mu^\mp 2\nu 2\bar{\nu}$ events, radiative Bhabha and μ -pair events, the $e^+e^- \rightarrow e^+e^-e^+e^-$ and $e^+e^- \rightarrow e^+e^-\mu^+\mu^-$ two-photon processes, and beam-gas interactions. In the p_e/E_B vs p_μ/E_B plane, where p_e/E_B (p_μ/E_B) is the ratio of the electron (muon) momentum to the beam energy in the CM frame, the distribution of e - μ signal events peaks at (1,1). Events must lie within a circle about that peak: namely we require $(p_e/E_B - 1)^2 + (p_\mu/E_B - 1)^2 < 0.01$. Figure 1 shows the distribution of $(p_e/E_B - 1)^2 + (p_\mu/E_B - 1)^2$ after all other selection criteria have been applied, for the signal, $\Upsilon(3S)$ data sample, and continuum backgrounds estimated from Run 6 data. The angle between the two lepton tracks in the CM is required to be more than 179° . In order to reduce continuum background from μ -pairs and to suppress Bhabha events in which an electron is misidentified as a muon because it passes through the space between crystals, the primary muon candidate is required to deposit at least 50 MeV in the EMC. We require that the lepton tracks fall within the angular acceptance ($24^\circ < \theta_{Lab} < 130^\circ$) of the EMC, where θ_{Lab} is the polar angle of lepton tracks in the lab frame.

The signal efficiency, as determined from signal MC, is $(23.42 \pm 0.13 \text{ (stat)})\%$. Figure 2 shows the $e\mu$ invariant mass distribution of the data candidates and background events, as well as the potential signal, after all selection requirements have been applied.

No events from the generic $\Upsilon(3S)$ MC sample survive the selection. We estimate an uncertainty of ± 0.9 events in this source of potentially misidentified generic $\Upsilon(3S)$ decays by loosening the PID selectors and use the uncertainty in the surviving number of events with this loosened selection as the uncertainty in this background. The determination of the continuum backgrounds obtained using the Run 6 data, as described above, predicts a background of 12.2 ± 2.1 events from continuum processes. The MC samples of the continuum are only used as a cross check on backgrounds at various stages of the analysis. No events from Bhabha, τ -pairs, $c\bar{c}$, $u\bar{u}+d\bar{d}+s\bar{s}$, or generic $\Upsilon(3S)$ MC pass the selection. The MC predicts that 0.16 ± 0.05 continuum μ -pair events survive the final

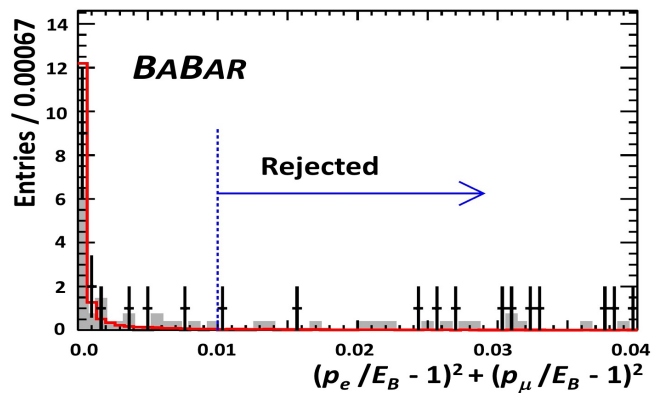


FIG. 1: Distribution of the squared distance from the point (1,1) in the plane of the scaled electron vs muon momenta for events satisfying all other selection criteria in the data (points with error bars), continuum background (gray histogram, from the Run 6 control sample normalized to 27.02 fb^{-1}), and simulated signal (red histogram, arbitrarily normalized). The dashed line indicates the position of the 0.01 requirement.

selection. An uncertainty of ± 2.3 events is assigned to the total background estimate, calculated as the quadrature sum of the uncertainties in the $\Upsilon(3S)$ and continuum background estimates.

Table I summarizes the signal efficiency, estimates of the numbers of background events, and numbers of events in the $\Upsilon(3S)$ data sample at the various stages of the selection.

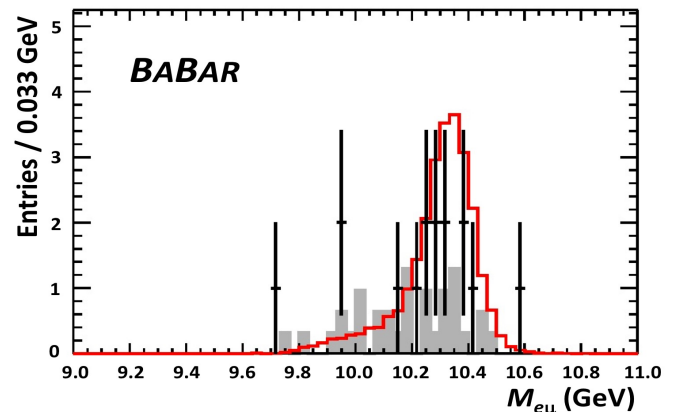


FIG. 2: The distribution of the $e\mu$ invariant mass of events surviving all selection criteria. The data sample is presented as the histogram in black with error bars and the open red histogram represents the signal MC with arbitrary normalization. The grey histogram shows the estimate of the continuum background from the Run 6 control sample data with the rate scaled to the amounts expected at 10.36 GeV for a data sample of 27.02 fb^{-1} and the mass scaled to $10.36/10.58$.

We assess the systematic uncertainties in the signal efficiency by determining the ratio of data to MC yields for

a control sample of $e^+e^- \rightarrow \tau^+\tau^- \rightarrow e^\pm\mu^\mp 2\nu 2\bar{\nu}$ events in an $e\mu$ mass sideband. For this study, we reverse the two major kinematic requirements, the E_B -normalized lepton momentum cut and the requirement on the angle between the two tracks, in order to obtain a large control sample of τ -pair events. This τ control sample study measures the systematic uncertainty associated with particle identification, tracking, kinematics, trigger selection criteria, and all other effects except those associated with the two major kinematic requirements used to select the control sample. Figure 3 shows the distribution of $M_{e\mu}$ for the data and MC in the τ control sample. We evaluate the associated correction to the signal efficiency by measuring the ratio $(N_{\text{Data}} - N_{\text{non-}\tau^+\tau^-}^{\text{MC}}) / N_{\tau^+\tau^-}^{\text{MC}}$ in the sideband region $6 \text{ GeV} < M_{e\mu} < 8 \text{ GeV}$, which is just below our signal region, where N_{Data} is the number of events in the data, $N_{\tau^+\tau^-}^{\text{MC}}$ is the number of τ -pair events predicted in MC, and $N_{\text{non-}\tau^+\tau^-}^{\text{MC}}$ the number of MC-predicted events that are not τ -pairs. We obtain a value of $1.007 \pm 0.010(\text{stat})$ for this ratio. We take the quadratic sum of the statistical uncertainty in this ratio and difference from unity as this part of the relative systematic uncertainty, 1.2%, in the signal efficiency. We evaluate the systematic uncertainties associated with the two major kinematic requirements that are reversed for the τ control sample selection by using them to select a μ -pair control sample having very similar kinematic properties as the signal. We conservatively vary the values of the two selection criteria from the default values and assign the differences in the selection efficiencies between MC and data for the μ -pair control samples as the relative efficiency uncertainties associated with these requirements. The E_B -normalized momentum requirement is varied by ± 0.0015 and the back-to-back angle requirement by $\pm 0.1^\circ$. The number of signal events remains unchanged under these variations. Table II summarizes the systematic uncertainties. The signal efficiency is $(23.4 \pm 0.8)\%$, where the quoted uncertainty is determined by summing in quadrature the individual contributions.

TABLE II: Summary of systematic uncertainties. The values of the efficiency, background, and number of $\Upsilon(3S)$ decays are presented in the first column and their uncertainties in the second column. The different contributions to the efficiency systematic uncertainties are also presented.

Component Value	Uncertainties by Source
Signal Efficiency: 0.2342	Lep. Mom. cut: 0.0068 (2.9 %)
	Back-to-back cut: 0.0026 (1.1 %)
	All other cuts: 0.0028 (1.2 %)
	MC statistics: 0.0003 (0.13 %)
	± 0.0078 (3.3 %)
$N_\Upsilon: 117.7 \times 10^6$	$\pm 1.2 \times 10^6$ (1.0 %)
BG: 12.2	± 2.3 (19 %)

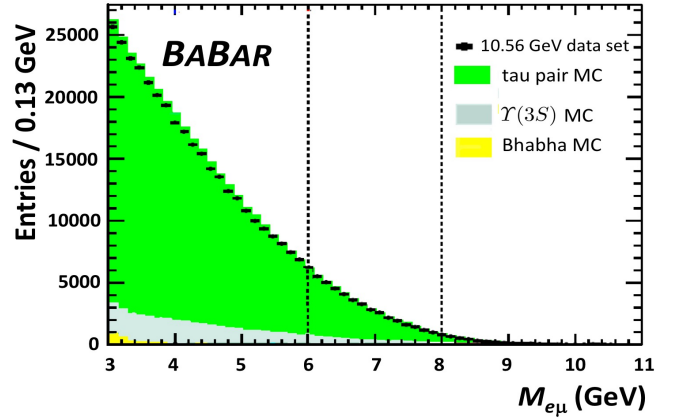


FIG. 3: The distribution of the $e\mu$ invariant mass of events in a control sample dominated by τ -pair events obtained by reversing the two major kinematic requirements in the selection. The green, light grey, and yellow colored histograms represent the MC predictions for $\tau^+\tau^-$, generic $\Upsilon(3S)$ decays, and Bhabha events, respectively, while the histogram represented by the black line with error bars represents data from the $\Upsilon(3S)$ data sample. The systematic uncertainty in the signal efficiency associated with all requirements but those on the two kinematic requirements used to define this sample is obtained by comparing the MC expectations with the data in the side-band region indicated by the dashed vertical lines.

After unblinding the data, we find $N_{\text{cand}}=15$ candidate events and have an expected background of 12.2 ± 2.3 events from a sample of $(117.7 \pm 1.2) \times 10^6$ $\Upsilon(3S)$ mesons. Calculating the branching fraction from $(N_{\text{cand}} - N_{\text{BG}}) / (\epsilon_{\text{sig}} N_{\Upsilon(3S)})$ gives:

$$\mathcal{B}(\Upsilon(3S) \rightarrow e^\pm\mu^\mp) = (1.0 \pm 1.4(\text{stat}) \pm 0.8(\text{syst})) \times 10^{-7} \quad (1)$$

where the statistical uncertainty is that from N_{cand} and all other uncertainties are included in the systematic uncertainty. As this result is consistent with no signal, we set an upper limit at 90% confidence level (CL) on the branching fraction by using the CLs method [15], a modified frequentist method that accommodates potential large downward fluctuations in backgrounds:

$$\mathcal{B}(\Upsilon(3S) \rightarrow e^\pm\mu^\mp) < 3.6 \times 10^{-7} \text{ @ 90\% CL.} \quad (2)$$

The CLs expected 90% CL upper limit, given the number of background events and assuming no signal, is 2.8×10^{-7} .

This result is the first reported experimental upper limit on $\Upsilon(3S) \rightarrow e^\pm\mu^\mp$ and from any $b\bar{b}$ bound state. It can be interpreted as a limit on NP using the relationship $(g_{NP}^2 / \Lambda_{NP})^2 / (4\pi\alpha_{3S}Q_b / M_{\Upsilon(3S)})^2 = \mathcal{B}(\Upsilon(3S) \rightarrow e\mu) / \mathcal{B}(\Upsilon(3S) \rightarrow \mu\mu)$, ignoring small kinematic factors, and where $Q_b = -1/3$ is the b -quark charge and α_{3S} is the fine structure constant at the $M_{\Upsilon(3S)}$ energy scale. Using the world average $\mathcal{B}(\Upsilon(3S) \rightarrow \mu^+\mu^-) = 2.18 \pm 0.21$ [1] gives a 90% CL upper limit of $\Lambda_{NP} / g_{NP}^2 > 80 \text{ TeV}$.

We are grateful for the excellent luminosity and machine conditions provided by our PEP-II colleagues, and for the substantial dedicated effort from the computing organizations that support *BABAR*. The collaborating institutions wish to thank SLAC for its support and kind hospitality. This work is supported by DOE and NSF (USA), NSERC (Canada), CEA and CNRS-IN2P3 (France), BMBF and DFG (Germany), INFN (Italy), FOM (The Netherlands), NFR (Norway), MES (Russia), MINECO (Spain), STFC (United Kingdom), BSF (USA-Israel). Individuals have received support from the Marie Curie EIF (European Union) and the A. P. Sloan Foundation (USA).

* Deceased

† Now at: Wuhan University, Wuhan 430072, China

‡ Now at: Università di Bologna and INFN Sezione di Bologna, I-47921 Rimini, Italy

§ Now at: King's College, London, WC2R 2LS, UK

¶ Now at: Western Kentucky University, Bowling Green, Kentucky 42101, USA

** Now at: University of Huddersfield, Huddersfield HD1 3DH, UK

†† Now at: University of South Alabama, Mobile, Alabama 36688, USA

‡‡ Also at: Università di Sassari, I-07100 Sassari, Italy

§§ Also at: Gran Sasso Science Institute, I-67100 L'Aquila,

Italy

- [1] P. A. Zyla *et al.* (Particle Data Group), PTEP **2020**, 083C01 (2020).
- [2] S. Nussinov, R. D. Peccei, and X. M. Zhang, Phys. Rev. D **63**, 016003 (2001).
- [3] U. Bellgardt *et al.* (SINDRUM Collaboration), Nucl. Phys. B **299**, 1 (1988).
- [4] T. Gutsche, J. C. Helo, S. Kovalenko, and V. E. Lyubovitskij, Phys. Rev. D **83**, 115015 (2011).
- [5] J.P. Lees *et al.* (*BABAR* Collaboration), Nucl. Instr. and Methods A **726**, 203 (2013).
- [6] J. R. Klein and A. Roodman, Annu. Rev. Nucl. Part. Sci., **55**, 141 (2005).
- [7] B. Aubert *et al.* (*BABAR* Collaboration), Nucl. Instr. and Methods A **479**, 1 (2002).
- [8] B. Aubert *et al.* (*BABAR* Collaboration), Nucl. Instr. and Methods A **729**, 615 (2013).
- [9] B. F. L. Ward, S. Jadach, Z. Was, Nucl. Phys. Proc. Suppl. **116**, 73 (2003).
- [10] S. Jadach, W. Placzek and B. F. L. Ward, Phys. Lett. B **390**, 298 (1997).
- [11] D. J. Lange, Nucl. Instr. and Methods A **462**, 152 (2001).
- [12] S. Agostinelli *et al.* (Geant4 Collaboration), Nucl. Instr. and Methods A **506**, 250 (2003).
- [13] T. G. Dietterich and G. Bakiri, Journal of Artificial Intelligence Research, **2**, 263 (1995).
- [14] I. Narsky, "Optimization of Signal Significance by Bagging Decision Trees", arXiv:physics/0507157.
- [15] A. L. Read, J. Phys. G **28**, 2693 (2002); G. Cowan, K. Cranmer, E. Gross, O. Vitells, Eur. Phys. J. C **71**, 1554 (2011), Erratum: Eur. Phys. J. C **73**, 2501 (2013).